Characterization of the long-term toxic response of proximal tubule epithelial cells in a microphysiological system

Yousif Issam Abuhamad

A thesis

submitted in partial fulfillment of the

requirements for the degree of

Master of Science

University of Washington

2024

Committee:

Edward Kelly

Catherine Yeung

Judit Marsillach

Program Authorized to Offer Degree:

Environmental and Occupational Health Sciences

University of Washington

Abstract

Characterization of the long-term toxic response of proximal tubule epithelial cells in a microphysiological system

Yousif Issam Abuhamad

Chair of the Supervisory Committee:

Edward Kelly

Department of Environmental and Occupational Health Sciences

Kidney diseases impact 850 million people globally, with 1 in 7 US adults affected, making it the 9th leading cause of death. Factors such as genetic variability, co-occurring health conditions, and exposure to drugs and environmental chemicals contribute to kidney diseases, which may take months or years to manifest clinically. Existing research lacks effective strategies, assays, and models for assessing human acute and chronic in vitro kidney toxicity, leading to research gaps in the nephrotoxicity of xenobiotics. Identification of potential kidney toxicants can help reduce the incidence of kidney disease. Organs-on-chips or microphysiological systems (MPS) are innovative microfluidic models to enhance our understanding of xenobiotic effects on kidney function. Previous studies from our group replicated toxic responses in kidney proximal tubule epithelial cells (PTECs); however, this was limited to acute

exposures (2-10 days). To assess the applicability of our PTEC MPS in chronic toxicity testing, we conducted temporal studies using 50 μM polymyxin B (PMB), a known kidney toxicant, at baseline and 2.5, 5, and 6 months after cell seeding. Toxic response was measured through kidney injury molecule-1 (KIM-1) and interleukin-6 (IL-6) concentrations in effluent, coupled with global transcriptome profiles. We observed a decrease over time in the magnitude of injury markers and genes of toxic exposure in response to acute PMB exposure. This suggests that response to toxicity decreases in older PTEC MPS devices; however, a toxic response was still detected. Furthermore, we cultured PTEC MPS devices beyond 6 months to determine the limits of PTEC MPS viability. The PTEC MPS have remained structurally stable for over 13 months as evaluated by brightfield microscopy. Our results suggest that PTEC MPS can potentially be used to evaluate chronic exposures for up to a year, given that a decrease in toxic response over time is considered. PTEC MPS can potentially be used for the prediction of nephrotoxicity by chronic exposure to low concentrations of xenobiotics.

Introduction

More than 850 million people are affected by kidney disease worldwide; this is two times more than people with diabetes and more than 20 times more than people with HIV/AIDS (Jager *et al.*, 2019). With a diverse range of causative factors and associated health complications, kidney disease poses a substantial threat to public health. Kidney disease is associated with exposure to a range of co-occurring health conditions, environmental toxicants, pathogens, and pharmaceutical products (Soderland *et al.*, 2010; Jha *et al.*, 2013).

Research on the etiology of kidney disease can potentially reduce its incidence by identifying harmful exposures, characterizing biological mechanisms, and discovering potential treatment options. Assessing the nephrotoxicity of chemicals currently requires animal studies or epidemiologic studies, both of which are time consuming and costly. Therefore, this requires new research strategies and models.

The use of in vitro kidney cell culture models provides an opportunity to contribute to toxicity assessments and chemical pathway analyses, while reducing the need for animal testing in toxicological research. One such model is microphysiological systems (MPS) also known as organ-on-a-chip. Kidney MPS culture human kidney cells in the tubule of a microfluidic device and exhibit structural and functional properties similar to human kidney cells in vivo. Many groups have successfully developed kidney MPS using primary human proximal tubule epithelial cell (PTECs) (Jang *et al.*, 2013; Wilmer *et al.*, 2016; Chang *et al.*, 2017; Van Ness *et al.*, 2017; Weber *et al.*, 2018; Lidberg *et al.*, 2022), the segment of the nephron with the highest xenobiotic exposure, and a high susceptibility to nephrotoxicity. PTEC MPS models can potentially be used as an in vitro human cell culture model which mimic aspects of kidney physiology that are lacking in animal models or 2D cell cultures. However, these systems have not been tested for extended periods of time, and we have little understanding of how cell viability and cell function changes over such durations.

Public health significance of chronic kidney disease

Chronic kidney disease (CKD) is a progressive condition characterized by the gradual loss of kidney function over time. CKD is defined clinically based on the presence of kidney damage or decreased kidney function for 3 months or more (Levey and Coresh, 2012). End stage kidney disease is characterized by kidney failure and requires dialysis or transplant for survival.

The global prevalence of CKD is estimated to be around 11 to 13%, with a higher burden of disease in less economically developed countries (Hill *et al.*, 2016). Compared to all diseases and injuries measured by the 2019 Global Burden of Disease Study, CKD ranks 18th in the number of disability-adjusted life years (DALYs) lost for all age groups. CKD has seen a marked increase in DALYs in recent years, indicating a worsening global burden of disease. This increase contrasts with other chronic diseases like ischemic heart disease, stroke, and liver cirrhosis, which have decreased over time (Vos *et al.*, 2020). The global prevalence of CKD coupled with its increasing incidence underscores its public health significance.

A major public health challenge of managing CKD is its diverse etiology. Loss of kidney function is associated with other diseases like chronic hypertension and diabetes, which are the leading causes of CKD in developed countries and many developing countries (Jha *et al.*, 2013). CKD is also associated with exposure to a range of environmental chemicals, pathogens, or pharmaceuticals. Nephrotoxic environmental chemicals include a range of heavy metals like

lead, cadmium, arsenic and mercury, as well as other toxicants like arsine gas, carbon tetrachloride and toluene. Exposure to these toxicants occurs both in industrial or occupational settings as well as through ingestion of contaminated food and water (Soderland *et al.*, 2010).

Symptoms of CKD do not manifest until 50% of kidney function is irreversibly lost; this is a public health challenge due to the insidious disease onset. At earlier stages of CKD, treatment options aim to delay end stage kidney disease (Turner *et al.*, 2012). However, the only treatment of end stage kidney disease is renal replacement therapy (Liyanage *et al.*, 2015). Dialysis and kidney transplant can heavily impact the quality of life of patients (Evans Roger W. *et al.*, 1985), and kidney transplants have limited availability. The insidious nature of CKD and its limited treatment options highlight the importance of managing modifiable behaviors and identifying unknown risk factors of CKD.

In Vitro Kidney Research

Given the escalating public health threat of CKD and our difficulty in detecting these compounds using traditional methods, innovative research approaches are important to help characterize the diverse etiology of CKD. In vitro cell cultures are a physiologically relevant, moderate throughout model to identify nephrotoxic agents, elucidate biological mechanisms and investigate interventions and treatments. While many in vitro models are currently used in researching CKD, more innovative approaches are needed to improve the accuracy of these models. In vitro cell cultures grow human or animal cells and can be used to evaluate cellular function in a controlled environment. Cell culture research on the nephrotoxicity of environmental chemicals and pharmaceutical products can help identify causative agents of CKD. In vitro toxicity research can potentially reduce the incidence of CKD through identifying nephrotoxic compounds. Historically, research on the nephrotoxicity of compounds relied mostly on animal models. Cell culture models can help replace or reduce animal studies, which is a goal of the principle of the 3Rs of animal testing (replace, reduce, and refine), which aims to improve laboratory animal welfare within toxicological and pharmaceutical testing. Cell culture models which use human cells are potentially more physiologically relevant in comparison to animal models, as they can recapitulate human genetics and physiology.

To effectively study CKD using cell culture models, it is essential to use an appropriate kidney cell type. Among the many cell types present in a kidney and nephron, proximal tubule cells are commonly used in CKD research as they play an important role in CKD pathogenesis.

Overview of the Proximal Tubule

The nephron is the functional unit of the kidney and is made up of two major structures: the glomerulus and the tubule **(Figure 1)**. The segments of the nephron include the proximal tubule, the loop of Henle, the collecting tubule, and the distal tubule. There are approximately 1 million nephrons in each human kidney. Proximal tubule cells can be grown in cell cultures to study some forms of CKD. The proximal tubule's main function is the reuptake of useful solutes (glucose, amino acids, bicarbonate, and minerals) from the filtrate of the glomerulus. The proximal tubule is also responsible for the uptake, biotransformation and secretion of toxicants, pharmaceuticals, and waste products, leading to high exposure in PTECs to these potentially

nephrotoxic compounds. The active transport in the proximal tubule leads to a high ATP requirement which is reflected in the high density of mitochondria in the proximal tubule (Hall and de Seigneux, 2022).

Human kidneys are highly susceptible to injury as kidney cells are exposed to a range of compounds due to their role in the removal of toxins from the body (Morrissey *et al.,* 2013). Furthermore, kidney cells have a limited regenerative capacity leading to reduced recovery after damage. Research indicates that damage to proximal tubule cells plays a major role in the onset and progression of some types of CKD (Waikar *et al.*, 2016; Liu *et al*., 2018; Chevalier, 2016).

Proximal Tubule Epithelial Cell Microphysiological Systems:

Traditional 2-D cell cultures models used in toxicological or pharmaceutical screening can be high throughput, well characterized models. However, screening accuracy may be impacted by a lack of physiologically relevant structures in 2-D cell cultures. Advancements in microfluidics, microfabrication and biomaterials have led to the development of MPS, or organs-on-a-chip. MPS are cell culture devices which culture cells in environments mimicking in vivo conditions. Physiological microenvironments are simulated in MPS using active media perfusion, 3D architecture, and biologically relevant interfaces. Cells grown in MPS tend to exhibit in vivo phenotypes not found in 2-D cell culture models (Wang *et al.,* 2018; Lelièvre, Kwok and Chittiboyina, 2017; Sánchez-Romero *et al.,* 2016; Kim and Takayama, 2015). Cells can be acquired from animal tissues, human donor tissues, or human induced pluripotent stem cells. MPS are a potentially useful tool for drug and toxicological testing, as they can be used as an ethical alternative or to supplement current methods like animal models. Many MPS do not interact with other cell types and organ systems, a reductionist approach can be used to characterize the functioning of a single cell type. However, multiple MPS can be connected using microfluidics, (Van Ness *et al.,* 2017) and replicate organ systems or metabolic processes which utilize multiple cell types. The biotechnology company Nortis, Inc. developed a microfluidic chip designed to replicate functional units of human tissues and organs (Tourovskaia *et al.*, 2014). The microfluidic chip is composed of polydimethylsiloxane (PDMS), a soft biologically compatible polymer. PDMS is optically transparent, which allows for in situ microscopy of the cells in the device. PDMS is also gas permeable, which provides cells with physiologically relevant oxygen conditions. The interior of the PDMS chip contains three 25 µL cylindrical culture chambers which are formed by casting collagen around a 120 µm glass fiber. 3D cell cultures can be seeded in the tubule, and media can be perfused using an external perfusion pump (Weber *et al.*, 2018). To promote cell adhesion, the tubule can be coated with collagen IV or another extracellular matrix (ECM) protein before cell seeding. Media containing nutrients for cell growth and maintenance is loaded into an inlet reservoir and flows through the lumen into an outlet reservoir. Flow rates can be set using the external perfusion pump. The MPS allows for analysis of effluent in the effluent media which can be used in a range of bioanalytical techniques. Cells can also be exposed to test compounds via the media.

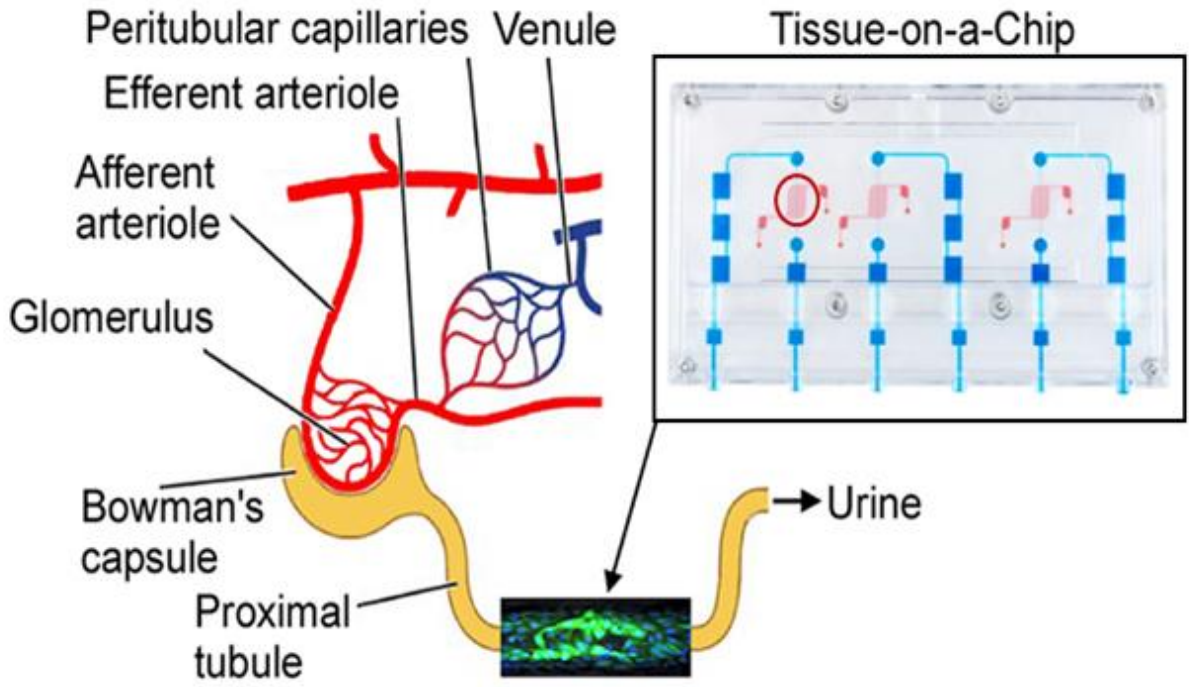

Figure 1) A schematic of a nephron and a microfluidic tissue-on-a-chip. Each chip contains three independent microtubules which can be seeded with proximal tubule cells. The stained microscopy image superimposed on the proximal tubule is an image of the microtubule in the MPS, stained with LIVE/DEAD stain and DAPI.

PTECs can be cultured in the Nortis MPS device, and cells in this “kidney-on-a-chip” demonstrate ciliated structures, cellular viability, and physiologically relevant morphology. The PTECs also exhibit apical-basal cell polarity, confirmed by the presence of polarized solute and drug transporters typical of proximal tubule cells, as well as apical localization of tight junction proteins (Weber *et al.,* 2016). Transporters recapitulated in the cells include OAT1, OAT3 and OCT2, and other SLC transporters, all of which are expressed in human proximal tubules in vivo. These physiologically relevant structures are due to the similarities to a human in vivo microenvironment (Wilmer *et al.*, 2016). For example, cells in the MPS device are exposed to physiologically relevant shear stress (about 1 dyne/cm^2) due to laminar flow of the media in the tubule. PTECs sense and react to differences in shear stress through changes in phenotype or organization, as well as changes in ion-transport capacity (Nieskens and Wilmer, 2016; Raghavan *et al.,* 2014). The mimicry of in vivo conditions causes the PTECs to exhibit a physiologically relevant phenotype and structure, allowing them to respond to biological insults and xenobiotics similarly to in vivo cells. This makes PTEC MPS a potentially useful tool for in vitro modeling. However, these MPS have not been tested for extended periods of time, making their applicability to chronic exposure modeling uncertain.

Aims of study

The goal of the study is to understand the sustainability and longevity of PTEC MPS for use in chronic exposure studies. The long-term applicability of MPS was assessed by analyzing the change in PTEC responses to toxicity over a 6-month period. The central hypothesis is that cellular responses after exposure to polymyxin B (PMB) are consistent over 2.5, 5 and 6 months. In our experiment, PMB was used to assess toxic response as PMB is an antibiotic which is known to be nephrotoxic (Weber *et al.*, 2018). The measure of toxic response is the concentration of the biomarker kidney injury molecule-1 (KIM-1). KIM-1 is a biomarker of injury and was collected and measured from the effluent media of the MPS. KIM-1 has traditionally been used as a marker of kidney injury and is shown to increase in response to PMB both in vivo (Babic *et al.*, 2017) and in MPS (Weber *et al.,* 2018). The concentration of the proinflammatory cytokine Interleukin 6 (IL-6) was also measured from effluent media. IL-6 has been demonstrated to increase in PTEC in response to inflammation (Su, Lei and Zhang, 2017). Treated and untreated cells underwent RNA sequencing analysis to evaluate gene expression patterns. We pursued this goal in the following specific aims:

Aim 1 is to demonstrate maintained toxic response through stable Kidney Injury Molecule-1 (KIM-1) secretion (±30%) compared to baseline with exposure to polymyxin B in at least 3 tubules at 2.5, 5, and 6 months.

Aim 2 is to demonstrate maintained expression of Interleukin 6 (IL-6) (±30%) compared to baseline with exposure to polymyxin B in at least 3 tubules at 2.5, 5, and 6 months.

Aim 3 is to demonstrate stable RNA transcriptome profiles in response to polymyxin B exposure in at least 3 tubules at 2.5, 5, and 6 months.

Aim 4 is to demonstrate extended cell viability via live-dead staining with >80% cell viability in at least 3 PTEC tubules at 2.5, 5, and 6 months.

The study can help establish PTEC MPS as a valid in vitro model to be used in chronic toxicity testing, as the long-term function of PTEC MPS is not well understood.

Methods

Study Overview:

To assess PTEC toxic response over time, the PTECs were exposed 50 µM PMB for 48 hours at 4 time points: 16 days (baseline), 2.5 months, 5 months, and 6 months. Effluent media was collected before exposure and 48 hours after exposure. Every three weeks, the media was changed to fill the inlet reservoir with sufficient media, effluent was collected during each media change. The effluent media was stored at -80ºC for future quantification of toxic response. The collected effluent was assayed for KIM-1 and IL-6. Effluent KIM-1 and IL-6 concentrations were determined using enzyme-linked immunosorbent assay (ELISA). RNA from the cells were collected for RNA Sequencing analysis 2 days after PMB treatment.

A total of 30 MPS devices were seeded with PTECs, with each device containing 3 lumen each. To reduce the chance of contamination, the cells were stored in a dedicated incubator, which was used only for this project.

Proximal Tubule Cell Isolation:

Kidney tissues were acquired from Novabiosis, the kidney was obtained as discarded tissue unsuitable for transplant from a deceased donor (Male, aged 73). The kidney tissue was received in dPBS^{++}/Pen-Strep media. Tissue processing and cell isolation was conducted as previously described (Weber *et al.*, 2018). Briefly, the tissue from the kidney cortex was finely minced in a biosafety cabinet, and then digested in 1 mg/mL of collagenase IV solution (Worthington Biochemical Corp LS00418) for 30 minutes at 37°C while being shaken. The digestion reaction was inhibited using 1:1 horse serum (Invitrogen, 26050-088) and the solution was vortexed, then allowed to settle to separate glomeruli and other tissue. The supernatant cell suspension was then centrifuged, washed in DPBS++ (Invitrogen, 14040133) and plated on T25 flasks with DMEM/F12 media (+) L-glutamine/15 mM HEPES (Invitrogen, 11330-032) supplemented with ITS-A Supplement (100x) (Invitrogen, 51300-044) and hydrocortisone (50 µM) (Sigma, H6909).

Cell Seeding:

The Nortis chip tubules were coated with human collagen type IV (rat tail) (Corning, 354249) to promote cell adhesion. Proximal tubule cell cultures with a confluency between 50-100% were selected for seeding into the chips. First the cells underwent trypsin digestion for 2 minutes at 37°C using a 0.005% trypsin-EDTA solution (Invitrogen, 25300-054). Cells were scraped from the flask using a cell scraper. After 7 minutes in the centrifuge at 1500 RPM, the supernatant was collected resuspended with a concentration of 20×10^6 cells/ml. The cells were injected into the injection port of the MPS and were incubated for 12 hours to allow for cell adhesion to the collagen matrix. After adhesion, flow was initiated at 0.5 µL/min. Cells were given 16 days of incubation before treatment.

The incubator can store and perfuse 24 chips at a time. After the 16-day timepoint, 6 MPS were removed after PMB treatment. So, 6 more chips were seeded and incubated to utilize any space in the incubator and increase the number of cell samples.

Media Change:

Media changes took place every 3 weeks, during which 20mL of media was added to the inlet reservoir of the Nortis MPS housing. The pneumatic system pumping media through the tubule had a flow rate of 0.5 µL/min. Media changes were completed in a biosafety cabinet. Furthermore, reservoirs were replaced during media changes to reduce the risk of bacterial or fungal contamination. 1.5 mL of effluent media was collected from the effluent reservoir of each tubule.

The media was composed of DMEM/F12 (Sigma, D5030), D glucose (Sigma, G8270), sodium bicarbonate buffer (Sigma, S5761), HEPES buffer (Gibco, 15630130), antibiotic-antimycotic solution (Gibco, 15240062), ITS -G (Gibco, 41400045) and hydrocortisone (50 µM) (Sigma, H6909)

Microscopy and Staining:

During each media change and during treatment, the tubules were examined under a Nikon TI-S microscope to qualitatively assess tubule viability. Light microscopy images were captured every 2 weeks for documentation.

After a 48-hour treatment, some tubules underwent LIVE/DEAD staining using the LIVE/DEAD Viability/Cytotoxicity Kit for mammalian cells (Molecular probes, L3224) according to the manufacturer's instructions. 5µL of calcein AM, 20µL EthD-1 and 20 drops of DAPI reagent were diluted in 10mL of sterile prewarmed DPBS++ and diffused into the tubule using a syringe pump via the outlet port at 0.5 µL/min at 37°C for 10 minutes. The cells were then perfused with DPBS++ at 10 µL/minute for 30 minutes to wash the cells, at 37°C under low light conditions.

Live cells were stained green by calcein AM and dead cells were stained red by ethidium homodimer-1 (EthD-1). The stain was used to qualitatively determine cell viability of control tubules. Cells were also exposed to NucBlue DAPI Reagent (Invitrogen, R37606) to stain nuclei blue.

ELISA:

Concentrations of KIM-1 and IL-6 were quantified using the Human TIM-1/KIM-1/HAVCR DuoSet ELISA kit (R&D Systems, DY1750B) and the Human IL-6 DuoSet ELISA kit (DY206-05, R&D Systems).

To determine KIM-1 and IL-6 concentrations from ELISA absorbance values, a standard curve was produced using the absorbance values of known standards. A 4-parameter logistic regression model (Hill model) was used to produce a standard curve for each plate. Any concentration values lower than the lowest standard were considered below the limit of detection, and the value was set at lower limit divided by the square root of two.

RNA Sequencing:

RNA was collected by injecting 100 µL of RLT buffer (Qiagen, 79216) into the upper section of the MPS lumen. The lysate was collected and stored at -80°C. The RNA extraction was

performed using an RNeasy Micro Kit (Qiagen,74004). The RNA was transcribed into cDNA in a PCR clean workstation using SMART-Seq v4 Ultra Low Input RNA Kit. The sequencing libraries were generated from the cDNA using the SMARTer ThruPLEX DNA-Seq kit. Sequencing was done by Novogene in paired end-mode, with 150 base pair reads. The library was quantified, and the library fragment lengths were verified using a Bioanalyzer instrument (Agilent Technologies). The base calls were produced using the NovaSeq 6000 instrument (RTA 3.1.5). The reads were then demultiplexed, and the unaligned BAM files were converted to FASTQ format using SamTools bam2fq (v1.4).

The RNA sequencing data was aligned to the database GENCODE human release 30 using STAR (v2.6.1d). The data was then processed further through R. The Bioconductor GenomicAlignments package was used to summarize the aligned data in counts per gene. The values were then adjusted using a trimmed mean of M-values normalization, to account for sequencing depth. The count data was then transformed into $\log_2$ counts per million (logCPM), all genes that are expressed at low levels (logCPM <0) throughout all samples were excluded. The mean variance relationship was calculated using the voom function in the Bioconductor limma package (Ritchie et al., 2015) This data was then fitted with a weighted linear regression model. Genes were selected as having a significant difference if there was a 20% change in expression and a false discovery rate < 0.05.

***Statistical Analysis*:**

All statistical analyses were done using R (R Core Team, 2023). Linear regression modeling coupled with ANOVA was used to assess the impact of PMB treatment on KIM-1 and IL-6 concentrations at different time points. A simple regression model was generated comparing KIM-1/IL-6 concentration and timepoint. Another similar model was created with PMB treatment group as a covariate. Linear regression modeling was used to assess the association between KIM-1 and IL-6 concentrations and cell age using effluent from control tubules. An ANOVA was used to compare the nested model. P values were generated using a paired t-test, comparing pretreatment and treatment KIM-1/IL-6 concentrations at the 6 months timepoint.

Statistical power calculations were performed on R using the pwr package to calculate the minimum sample size to show significance. A previous study measured the change in effluent KIM-1 from PTEC MPS following exposure to 50 µM PMB (Weber *et al.*, 2018). Mean KIM-1 concentrations and a pooled standard deviation was used to calculate an effect size for the power calculation. The power calculation determined that a sample size of 3 paired observations per group is needed to achieve a power of 0.8 at a significance level of 0.05 for detecting the observed effect size.

Results

Effect of PMB Treatment on Effluent KIM-1 Concentration

To assess the toxic response of the PTECs to 50 µM PMB at multiple time points (16 days, 2.5 months, 5, and 6 months), the biomarker of injury KIM-1 was measured in effluent before and after PMB treatment. Due to tubule loss, there was a low sample size at a few timepoints.

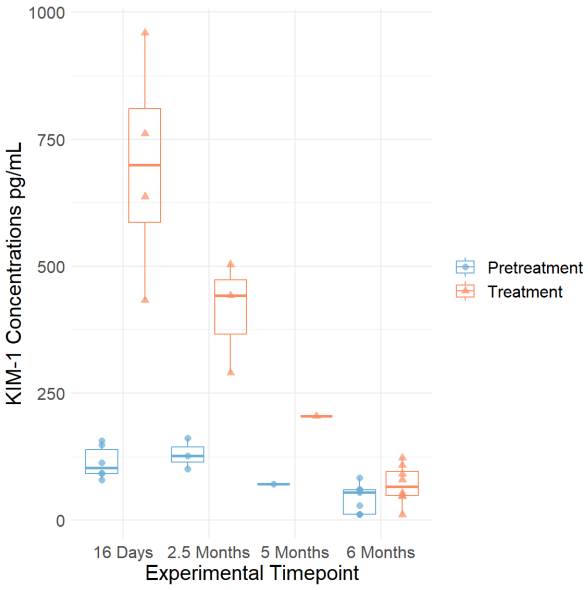

Figure 2) Boxplot of PMB pretreatment and treatment effluent KIM-1 concentrations at each timepoint. Cells were treated with PMB for 48 hours.

KIM-1 tends to decrease as cell age increases. Table 1 shows KIM-1 concentrations after PMB treatment: a 6-fold increase at 16 days, 4-fold at 2.5 months, 67% ($p < 0.01$) at 6 months, and 5-fold at 5 months (though only one tubule was treated at 5 months, reducing significance). The percent change in mean KIM-1 concentration is over 30% greater at all time points compared to 16 days. Pretreatment KIM-1 effluent at 6 months was slightly lower than other pretreatment concentrations. An ANOVA comparing two models, with and without PMB treatment, indicated a significant impact of PMB treatment on KIM-1 concentration at all time points.

Table 1: Summary statistics of KIM-1 effluent concentration

Time Point	Treatment	Mean KIM-1 Concentration (pg/mL)	Standard Deviation (pg/mL)	Number of tubules	Absolute difference in mean KIM-1 concentration (pg/mL)	Percent Change in mean KIM-1 concentration (%)
16 Days	Pretreatment	96.2	56.2	6	501.6	521.6
	Treatment	597.8	79.4	5		
2.5 Months	Pretreatment	100.2	49.4	3	326.0	325.2
	Treatment	426.2	115.1	3		
5 Months	Pretreatment	22.1	*NA*	1	101.1	457.0
	Treatment	123.2	*NA*	1		
6 Months	Pretreatment	42.0	27.1	9	28.2	67.1
	Treatment	70.2	36.9	8		

A multivariate linear regression model comparing KIM-1 concentration to the experimental timepoint with PMB treatment as a covariate was created. The model predicts a statistically significant difference in KIM-1 concentrations between treatment and pretreatment groups at 2.5 months and 6 months compared to baseline ($p < 0.001$). Furthermore, the linear regression model indicated a non-significant difference between KIM-1 concentration and experimental timepoint ($p = 0.07$). The small sample size decreases the accuracy of the multivariate regression model.

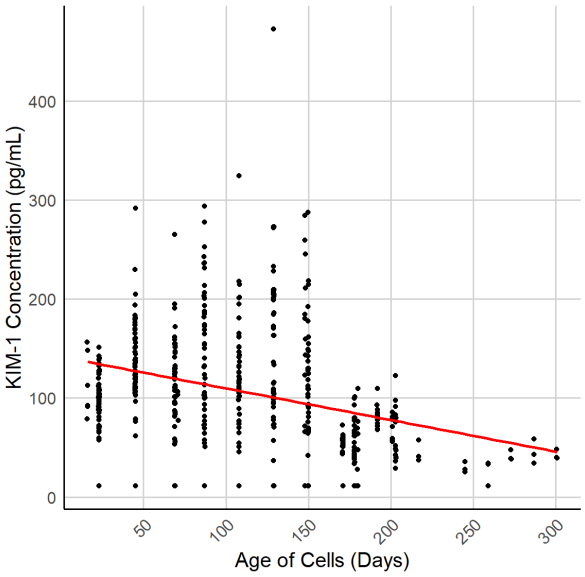

Figure 3) Scatterplot of effluent KIM-1 concentration (pg/mL) from control tubules and cell age in days $R^2 = 0.10$

Figure 3 shows effluent KIM-1 concentrations over time from untreated control tubules. The effluent KIM-1 concentration decreases slightly in older cells, similarly to pretreatment cells in Figure 2. A linear regression model comparing effluent KIM-1 concentration and cell age was generated. The model indicates a statistically significant decrease in KIM-1 concentration as cell age increases, with a decrease of 0.32 pg/mL of KIM-1 per day ($p < 0.001$, $n = 504$). Further regression modeling and an ANOVA was used to assess the role of plate-to-plate variation in the data. The prior KIM-1 concentration linear regression model was compared to another linear regression model which includes ELISA plate number as a covariate. The ANOVA p-value was below 0.01 suggesting an association between plate and measured KIM-1 concentrations.

Effect of PMB Treatment on Effluent IL-6 Concentration

To assess the toxic response of the PTECs to 50 μM PMB at multiple time points (16 days, 2.5 months, 5, and 6 months), the inflammatory biomarker IL-6 was measured in effluent before and after PMB treatment. Due to tubule loss, there was a low sample size at some timepoints.

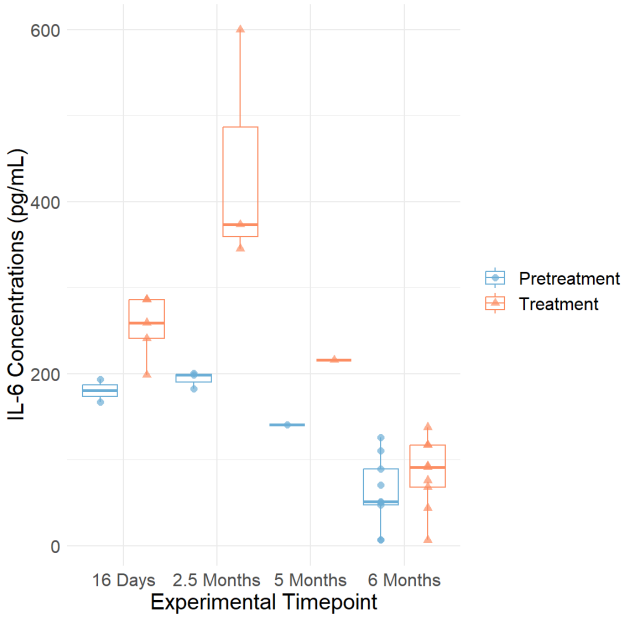

Figure 4) Boxplot of PMB pretreatment and treatment effluent IL-6 concentrations at each timepoint. Cells were treated with PMB for 48 hours.

IL-6 tends to decrease as cell age increases. Table 2 shows IL-6 concentrations after PMB treatment: A 41% at 16 days, 125% increase 2.5 months, 34% ($p = 0.22$) at 6 months, and 53% increase at 5 months (though only one tubule was treated at 5 months, reducing significance). The difference between the percent change in mean IL-6 concentrations between 16 days and 6 months is 15%. Pretreatment IL-6 effluent at 6 months was slightly lower than other pretreatment concentrations. An ANOVA comparing two models, with and without PMB treatment, indicated a significant impact of PMB treatment on IL-6 concentration at all time points.

Table 2: Summary statistics of IL-6 effluent concentration

Time Point	Treatment	Mean KIM-1 Concentration (pg/mL)	Standard Deviation (pg/mL)	Number of tubules	Absolute difference in mean IL-6 concentration (pg/mL)	Percent Change in mean IL-6 concentration (%)
16 Days	Pretreatment	180.4	18.5	2	74.0	41.0
	Treatment	254.3	36.6	5		
2.5 Months	Pretreatment	193.7	9.9	3	246.0	127.0
	Treatment	439.7	139.6	3		
5 Months	Pretreatment	140.7	*NA*	1	75.3	53.5
	Treatment	216.1	*NA*	1		
6 Months	Pretreatment	62.0	41.6	9	21.4	34.6
	Treatment	83.5	40.6	9		

A multivariate linear regression model comparing KIM-1 concentration to the experimental timepoint with PMB treatment as a covariate was built. The model predicts a non-statistically significant association between PMB treatment and an increase of KIM-1 concentration at all timepoints compared to 16 days ($p = 0.11$). The linear regression model predicts a non-significant change in KIM-1 concentration between 2.5 months and 16 days ($p = 0.78$), and a significant change in KIM-1 concentration between 6 months and 16 days ($p < 0.05$). However, the small sample size decreases the accuracy of the multivariate regression model.

In comparison to the KIM-1 concentration data, there are smaller absolute and percent changes in IL-6 concentration. There is also not a clear decreasing trend like in the KIM-1 data, the 2.5-month timepoint exhibited a larger IL-6 toxic response than at 16 days. The mean 6-month pretreatment KIM-1 concentrations were lower than pretreatment concentration at other timepoints. This is similar to the IL-6 6-month pretreatment concentration.

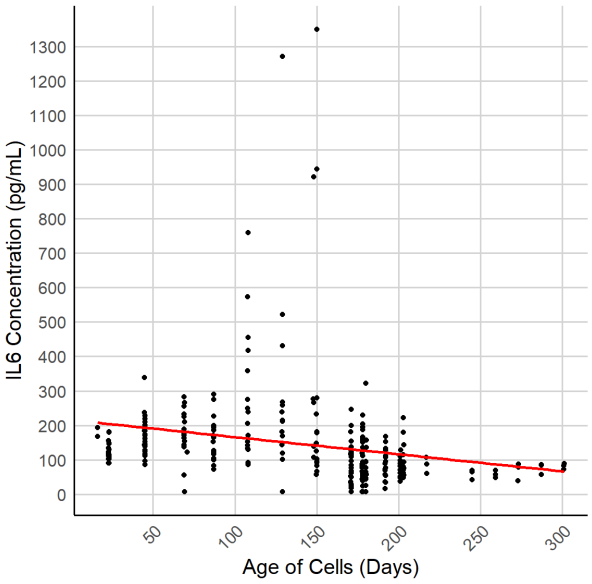

Figure 5) Scatterplot of effluent IL-6 concentration (pg/mL) and cell age in days from control tubules $R^2 = 0.10$

Figure 5 shows effluent IL-6 concentrations over time from untreated control tubules. The effluent IL-6 concentration decreases slightly in older cells, similarly to pretreatment cells in Figure 4. A linear regression model comparing effluent IL-6 concentration and cell age was generated. The model indicates a statistically significant decrease in KIM-1 concentration as cell age increases, with a decrease of 0.50 pg/mL of IL-6 per day ($p < 0.001$, $n = 266$). Further regression modeling and an ANOVA was used to assess the role of plate-to-plate variation in the data. The prior IL-6 concentration linear regression model was compared to another linear regression model which includes ELISA plate number as a covariate using an ANOVA. Similarly to the KIM-1 modeling, the ANOVA p-value was below 0.01 suggesting an association between plate and measured IL-6 concentrations. However, there is a correlation between plate number and cell age, as samples were not evenly distributed by timepoint on the ELISA plates. This suggests that the significant p-value comparing the models might not be significant due to plate-to-plate variation, but due to the experimental setup.

Effect of PMB Exposure on RNA Expression

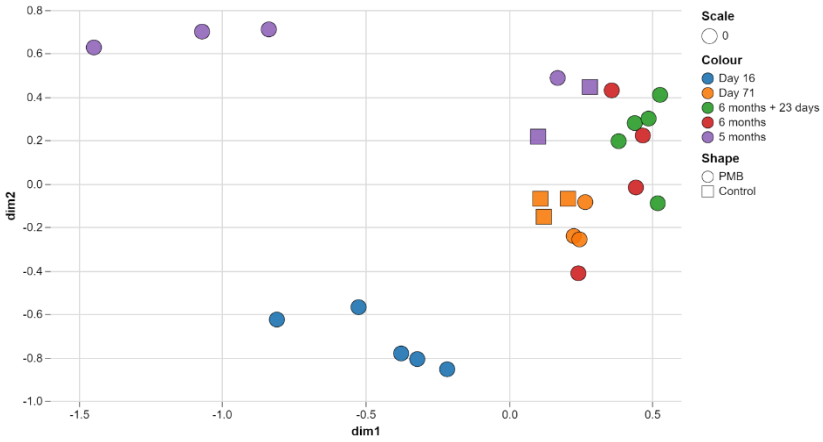

Figure 6) Principal Component Analysis (PCA) plot of RNA-Sequencing profiles comparing treatment group and experimental timepoint.

RNA sequencing was used to evaluate differences in RNA expression between time points and treatment groups. Principal component analysis (PCA) showed general clustering of the 2.5-month, 5-month, and 6-month timepoints. The 2.5-month timepoint (Day 71) data clustered tightly, regardless of treatment. However, the 5-month timepoint has large separation between the treatment groups along the first dimension. Day 16 treatment data points clustered together separately from the other datapoints, indicating a different RNA transcriptomic profile compared to later time points. Due to limitations on the number of MPS devices, there are few control groups we can compare with treatments. Regardless of timepoint, the control values clustered relatively close together. Ultimately, the PCA plot suggests that cells at later timepoints had different transcriptomic profiles than the cells at 16 days. The PCA plot also suggests a transcriptomic response to PMB at 5 months, but that response is not present in the 2.5-month timepoint. A total of 24% of the variance was explained by principal component 1, and 19% of the variance was explained by principal component 2.

Figure 7 highlights the change in RNA expression in selected genes of interest over time. As shown in Figure 7 and Table 3, we observed statistically significant upregulation of all genes in the metallothionein protein family (MT1G, MT1H, MT1M, MT1X, MT2A, MT1E, and MT1F) at 16 days, 2.5 months and at 6 months, without significant changes in the 5 months category (with the exception of MT2A). HMG-CoA reductase (HMGCR) and HMG-CoA synthase (HMGCS), genes in the pathway of cholesterol biosynthesis, were significantly upregulated at 16 days and 2.5 months, but not at later time points. Significant upregulation of heme oxygenase 1 (HMOX1) only occurred at the 16-day timepoint, and a significant downregulation of ATP-binding cassette transporter (ABCA1) occurred only at the 16-day timepoint. These results suggest that cells at 16 days respond to PMB through changes in transcription, this change is not reflected in later timepoints, except for upregulation of MT genes at 6 months.

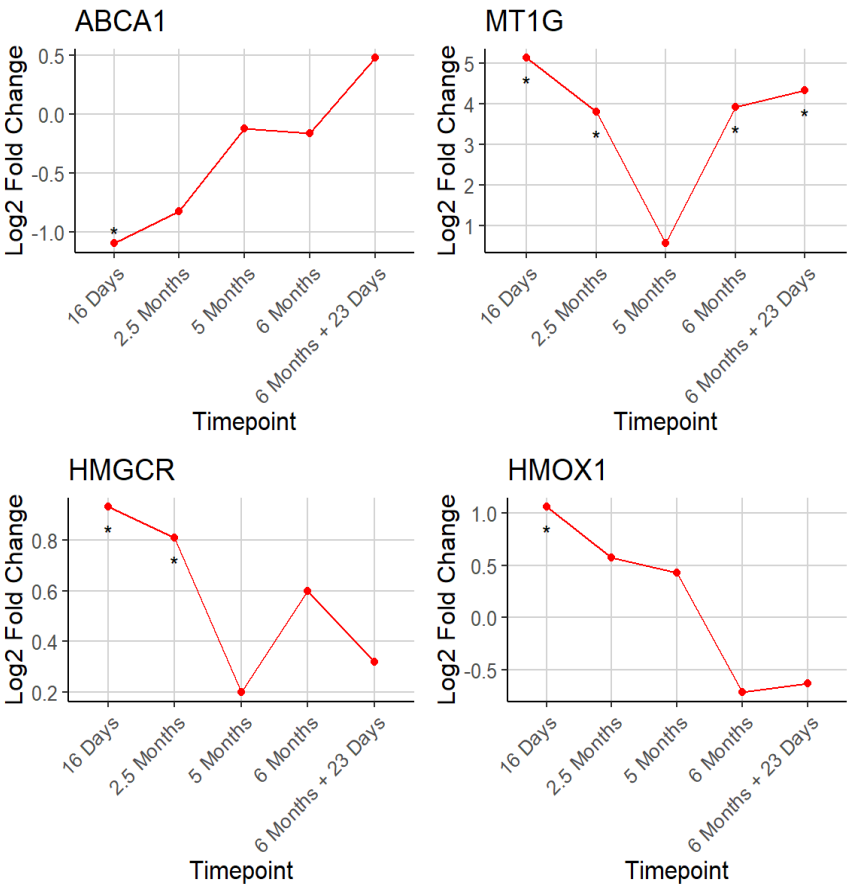

Figure 7) Line plots of Log2 Fold Change of selected genes comparing treatment to control tubules at each timepoint. * p < 0.01

Table 3: Log_2 fold change values of selected genes comparing treatments to controls.

Gene	Log_2 fold change				
	16 Days	2.5 Months	5 Months	6 Months	6 months +23 Days
MT1G	5.13*	3.80*	0.56	3.93*	4.34*
MT1H	5.09*	3.95*	0.85	4.53*	4.89*
MT1M	4.04*	2.91*	0.44	3.48*	3.82*
MT1X	3.20*	2.27*	0.49	1.77*	2.19*
MT2A	2.27*	1.69*	1.23*	1.81*	1.91*
MT1E	2.39*	1.62*	0.94	1.65*	1.90*
MT1F	2.50*	1.72*	0.27	1.58*	2.04*
HMGCR	0.93*	0.81*	0.20	0.60	0.32
HMGCS	1.54*	1.50*	0.25	0.99	0.48
HMOX1	1.06*	0.57	0.43	-0.72	-0.63
ABCA1	-1.10*	-0.83	-0.12	-0.16	0.48

* p < 0.01

Due to limitations in samples, some timepoints did not have control groups at the same timepoint. Some treatment samples were compared to control groups from other timepoints. As shown in figure 6, there were a low number of control groups, with only 2 for 5 months and 3 for 2.5 months, this limits the power to identify true differences. Because there were no controls for the 16 day and 6-month time points, the 16 days and 6-month treatment groups were compared to the 2.5 month and 5-month control groups respectively.

Cell Viability

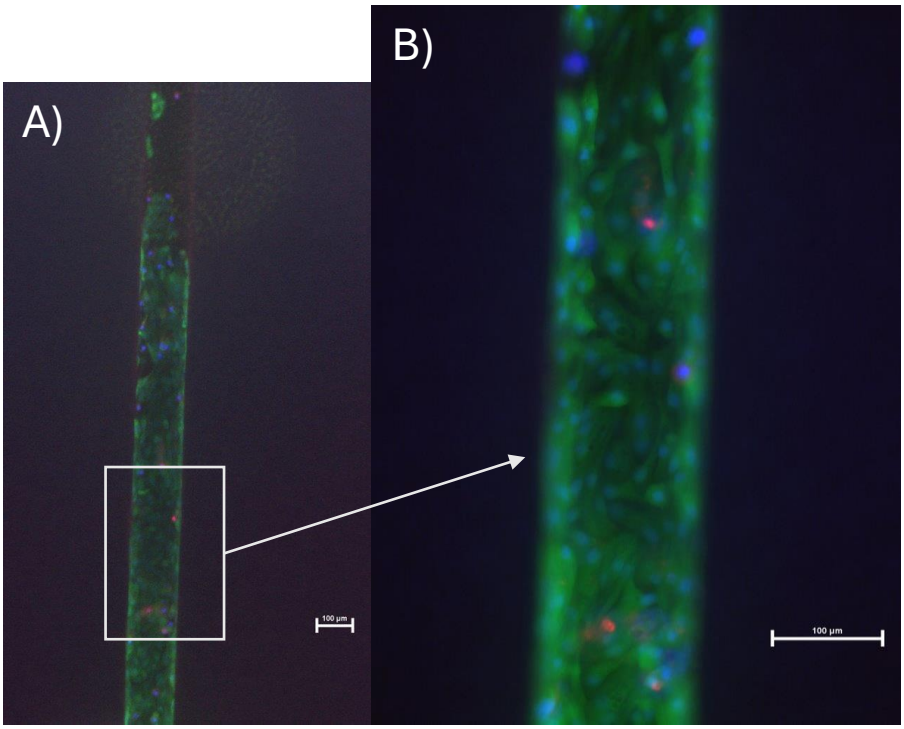

Cell viability at 6 months was determined by light microscopy with LIVE/DEAD and DAPI staining. Figure 8 showcases viable tubules at 6 months. The high proportion of green stained cells indicates that most PTECs in the tubule are alive and viable. Only a few dead cells are present in the tubule as indicated by red stains. The blue DAPI stains highlight nuclei in the tubule.

Figure 8) A) 6-month Timepoint LIVE/DEAD Stain and DAPI (4X), B) 6-month Timepoint LIVE/DEAD Stain and DAPI (10X).

Discussion

The results indicate that PTECs in MPS devices have lower responses to toxic stimuli at later timepoints. The change in effluent KIM-1 and IL-6 concentration in effluent decreased in older cells. Similarly, RNA expression of toxic response genes tended to decrease in later timepoints.

In both the control and treatment cells, effluent KIM-1 and IL-6 concentrations decreased with age. The decrease in IL-6 did not follow the same trend as KIM-1, because the change in IL-6 was greater in the 2.5-month timepoint than in the 16-day timepoint. This non-linear trend may stem from variation due to the low sample size or differences in the biological mechanism of KIM-1 and IL-6. The decrease in both KIM-1 and IL-6 secretion could be attributed to a range of factors. The number of cells may have decreased in older MPS devices, leading to lower biomarker secretion. Cells grown in MPS for long periods of time may down-regulate toxic

response pathways, as the cells are not exposed to any toxic insults or stressors. The prolonged absence of stressors in vitro may play a role in a decreased toxic response in older cells. Treating cells with low levels of PMB may help alleviate that potential downregulation, this could be explored in further research. Linear regression models of control data, combined with ANOVA, indicate a statistically significant variation between ELISA plates. However, samples were not evenly distributed by timepoint on the ELISA plates. This suggests that the significant p-value comparing the models may not be solely attributable to plate-to-plate variation, but rather to the experimental setup.

There was a decrease in KIM-1 and IL-6 expression over time. However, biomarkers of toxicity in older cells still increased, but at a smaller magnitude than younger cells. There was a 67% increase ($p < 0.01$) in effluent KIM-1 concentrations in the 6 months cells, and a 34% increase ($p = 0.22$) in effluent IL-6 concentration at 6 months. The change in KIM-1 is statistically significant as determined by a paired t-test, however the change in IL-6 concentration was not statistically significant. This increase suggests that cells at 6 months still respond to PMB exposure through secretion of KIM-1, with IL-6 being a less relevant biomarker. Statistical power analysis indicated that a sample size of 3 was needed to achieve a power of 0.8 at a significance level of 0.05. However, the effect size was determined from previous data with PMB exposure at 16 days (Weber *et al.*, 2018). The change in KIM-1 concentration decreased over time, meaning that the sample size of 3 might not be applicable at later timepoints. This assumption was confirmed through an ad hoc power calculation conducted using the 6 months KIM-1 concentration values. The calculation indicates a sample size of 22 was required to achieve a power of 0.8 at a significance level of 0.05, which is greater than the experimental sample size. Ultimately, PTEC MPS could be applied as a model for assessing the nephrotoxicity of compounds using a percentage increase in biomarkers of injury as opposed to an absolute increase. Limitations in sample size make it difficult to assess the statistical significance of biomarker changes at later timepoints. Toxicity assessments at 6 months using PTEC MPS should have a larger sample size due to the decrease in toxic response in those timepoints.

The results from the RNA sequencing analysis showed a similar pattern to the KIM-1 and IL-6 secretion data. At 16 days, a range of genes were affected by PMB exposure. These genes are present in detoxification or toxic response pathways, as well as hypothesized pathways of PMB toxicity. However, at later timepoints, the change in the genes of interest was not statistically significant. Drawing conclusions from the RNA sequencing data is challenging, as a lack of control tubules at 16 days and 6 months made comparing treatment and control groups challenging. The limited sample size makes it difficult to determine whether differences in gene expression are attributable to PMB exposure or to random variation. The PCA plot highlighted three distinct groups: 16-day treatment tubules, 5-month treatment tubules, and the remainder of the tubules. The grouping of the 2.5-month treatment and control groups suggests that even at 2.5 months, PMB has little effect on RNA expression at that timepoint. However, a range of genes of interest were significantly upregulated at 2.5 months. At 5 months, genes in the PMB response or detoxification pathways were not significantly affected by PMB treatment. Genes in the metallothionein family were significantly upregulated at all time points except for at 5 months, and HMGCR and HMGCS experienced a similar drop in RNA expression at 5 months. The decrease in the metallothionein genes, HMGCS and HMGCR does not follow the trend of other timepoints, as illustrated by figure 7. At 6 months, genes in the metallothionein family were upregulated following PMB exposure, while other genes did not change significantly. Metallothionein could be a potential measure of toxic response in a PTEC MPS to PMB, as they were consistently upregulated at earlier and later time points apart from 5 months. Ultimately, the RNA sequencing data tended to agree with the change in KIM-1 and IL-6 in response to

PMB over time, suggesting that older cells will have a smaller response to toxicity. Since RNA expression was calculated as a fold change, this decrease is likely not due to a lower cell number at later time points. This supports the hypothesis that quiescent cells may downregulate toxic response pathways in the absence of toxic stressors. Whilst the RNA sequencing data indicates a general decrease in toxic response, these changes were not consistent at all timepoints, and limitations in sample size make it difficult to reach any solid conclusions using RNA sequencing.

Overall, comparing PMB-treated tubules to untreated tubules through effluent KIM-1 concentrations, effluent IL-6 concentrations and RNA expression suggest that PTECs decrease their response to toxic stimuli over time, but a response is still present at 6 months. The results still suggest that PTECs in MPS devices could be used for chronic toxicity testing; however, the response decreases at later timepoints. The statistical significance testing suggests that KIM-1 is a more relevant biomarker of PMB toxicity in PTEC MPS. However, the ad hoc power calculation suggests that the sample size for KIM-1 was inadequate to determine a statistically significance difference in effluent KIM-1 concentration following treatment at 6 months.

A significant finding of the study was that PTECs could grow in an MPS device for up to 6 months. After 6 months, a few tubules were maintained indefinitely to assess the limit that PTECs could survive in MPS devices. The cells in the MPS device managed to survive up to 404 days, which is the longest PTECs have been maintained in a MPS to our knowledge. Cell survival was determined through light microscopy. Throughout the experiment, tubules were lost due to a range of factors including cell death, loss of flow, air bubbles, delamination of the collagen and bacterial or fungal contamination. This loss of tubules limited the sample size. Improvements in cell survival can improve the applicability of PTEC MPS in chronic studies. The survival of the cells for over a year indicates the stability of the model and highlights the potential of PTEC MPS as a robust platform for long-term in vitro studies.

In the context of CKD research, the results indicate that PTEC MPS could be used to assess the chronic toxicity of compounds. Further research on nephrotoxicity of compounds can help identify toxicants which damage proximal tubule cells. A validated PTEC MPS model can aid public health practitioners and regulators through identifying environmental contaminants, occupational chemicals, and pharmaceutical products which may contribute to the burden of CKD. However, the decrease in toxic response overtime impacts the applicability of the model at later timepoints. More research on the factors which lead to the decrease in toxic response may help in improving the model. A potential public health application of PTEC MPS is that it could be used as an accelerated human aging model. The 6-month phenomenon of cells decreasing in expression may replicate human aging, and MPS cell cultures could be used to simulate years of human aging in relatively less time. Further validation on the accuracy for MPS as an accelerated human aging model is required, but it could be a valuable potential tool for chronic exposure studies.

MPS is a relatively novel technology, so previous work on the model is limited. However, Weber et al studied the toxic response of PTECs to acute PMB exposure in a Nortis MPS (Weber *et al.*, 2018). The research group grew PTECs in an MPS device for 16 days, and then exposed the PTECs to PMB for 48 hours, similarly to our methodology. The study differs from ours because they only studied cells for up to 16 days, instead of 6 months. They measured effluent KIM-1 levels and reported an average pretreatment KIM-1 concentration of 151.2 ± 42.8 pg/mL and an average treatment concentration of 441.5 ± 112.3 pg/mL across 8 donors. This is comparable to our effluent KIM-1 concentration data, with a pretreatment concentration of 96.2 ± 56.2 pg/mL

and a treatment concentration of 597.8 ± 79.4 pg/mL. The data in Weber *et al.* had a large amount of variation between donors, with a range of 325.9 pg/mL for the averages of the pretreatment groups, and a range of 659.3 pg/mL for the averages in the treatment groups. This highlights the importance of using multiple donors, as donor-donor variation can lead to vastly different KIM-1 concentration.

Weber et al also compared the RNA expression between treatment and pretreatment groups through RNA sequencing. The research group identified key genes that were upregulated in response to PMB exposure in PTECs grown in a MPS (Weber *et al.,* 2018). Significantly upregulated genes of interest include the metallothionein protein family, HMOX1, HMGCR and HMGCS. ABCA1 was significantly downregulated in their data. Genes in the canonical antioxidant response pathway (e.g., NQO1, GCLM, and GPX) were not significantly induced following PMB response. This RNA expression was replicated in our 16-day PTEC MPS, with statistically significant increases in metallothionein protein genes, HMOX1, HMGCR and HMGCS. ABAC1 was significantly downregulated in our data, and genes in the antioxidant response pathway were similarly not significantly induced at 16 days.

The similarities in KIM-1 concentration between our data and the data reported by Weber et al support the results generated in this study and help alleviate the uncertainty caused by our low sample size. Furthermore, the replicability in the RNA-seq data improves the relevance and reliability of our results. The replicability suggests that even with different donors and different users, PTECs grown in MPS react to PMB in reproducible ways. This supports PTEC MPS devices as a reproducible model for use in toxicity testing at 16 days.

Study limitations: The inability to control cell number or cell density in the tubules is a limitation of this study, as it is difficult to determine if decreases in biomarkers are attributed to decreases in cell count, or biological mechanisms. Another limitation is that cells can survive in the injection port of the MPS devices, which can secrete biomarkers into effluent media and exhibit a different phenotype to cells in the tubule. The low sample size and single donor are also limitations of the study and impacts the statistical power of the data. A strength of the study is that it is innovative. MPS devices are a novel technology, and the PTECs remained viable for over a year, which is the longest PTECs were cultured in a MPS to our knowledge. Another strength is the reproducibility of the study; similar KIM-1 concentrations and RNA sequencing profiles to Weber et al highlight the reproducibility of our study.

Strengths of the Study: Future directions for PTEC MPS research could be focused on validating the model for use in toxicity testing. Now that the longevity of PTEC MPS is confirmed, a future study could assess the effects of exposure to a chronic low-level concentration of PMB, followed by a recovery period. A recovery period can be used to see whether PTEC toxic response biomarkers would return to baseline following a cessation of toxic exposure. Research on phenotypic changes of PTECs following PMB exposure can be used to elucidate the mechanism of PMB toxicity and compare the phenotypic changes in the model to in vivo disease state phenotypes. Further research could center on reducing PTEC MPS tubule loss, as this was a limitation of this study. Exploring strategies to mitigate PTEC MPS tubule loss could involve assessing the effectiveness of supplements to the media, or by changing the composition or physical design of the MPS device.

Conclusion

The feasibility of PTEC MPS as a chronic toxicity model was evaluated. PTEC's response over time to PMB toxicity was assessed through effluent KIM-1 concentration, effluent IL-6 concentration, and RNA sequencing. Effluent KIM-1 and IL-6 concentrations showed a general trend of decreasing over time. RNA sequencing analysis revealed decreased expression of selected toxic response genes in older cells. Nevertheless, effluent KIM-1 concentration still increased at 6 months following PMB exposure, suggesting that PTEC MPS can still be a viable toxicity model at 6 months if this decline in expression is factored into the analysis. IL-6 may be a less suitable biomarker. The findings underscore the potential of PTEC MPS as a robust model for chronic toxicity assessment, capable of aiding efforts to mitigate the public health impact of CKD by identifying nephrotoxic compounds.

References

Babic, J.T. *et al.* (2017) 'Evaluation of Urinary KIM-1 for Prediction of Polymyxin B-Induced Nephrotoxicity', *Antimicrobial Agents and Chemotherapy*, 61(11), pp. e01735-17. Available at: https://doi.org/10.1128/AAC.01735-17.

Chang, S.-Y. *et al.* (2017) 'Human liver-kidney model elucidates the mechanisms of aristolochic acid nephrotoxicity', *JCI Insight*, 2(22), p. e95978. Available at: https://doi.org/10.1172/jci.insight.95978.

Chevalier, R.L. (2016) 'The proximal tubule is the primary target of injury and progression of kidney disease: role of the glomerulotubular junction', *American Journal of Physiology-Renal Physiology*, 311(1), pp. F145–F161. Available at: https://doi.org/10.1152/ajprenal.00164.2016.

Evans Roger W. *et al.* (1985) 'The Quality of Life of Patients with End-Stage Renal Disease', *New England Journal of Medicine*, 312(9), pp. 553–559. Available at: https://doi.org/10.1056/NEJM198502283120905.

Hall, A.M. and de Seigneux, S. (2022) 'Metabolic mechanisms of acute proximal tubular injury', *Pflügers Archiv - European Journal of Physiology*, 474(8), pp. 813–827. Available at: https://doi.org/10.1007/s00424-022-02701-y.

Hill, N.R. *et al.* (2016) 'Global Prevalence of Chronic Kidney Disease – A Systematic Review and Meta-Analysis', *PLOS ONE*, 11(7), p. e0158765. Available at: https://doi.org/10.1371/journal.pone.0158765.

Jager, K.J. *et al.* (2019) 'A single number for advocacy and communication—worldwide more than 850 million individuals have kidney diseases', *Kidney International*, 96(5), pp. 1048–1050. Available at: https://doi.org/10.1016/j.kint.2019.07.012.

Jang, K.-J. *et al.* (2013) 'Human kidney proximal tubule-on-a-chip for drug transport and nephrotoxicity assessment', *Integrative Biology*, 5(9), pp. 1119–1129. Available at: https://doi.org/10.1039/c3ib40049b.

Jha, V. *et al.* (2013) 'Chronic kidney disease: global dimension and perspectives', *The Lancet*, 382(9888), pp. 260–272. Available at: https://doi.org/10.1016/S0140-6736(13)60687-X.

Kim, S. and Takayama, S. (2015) 'Organ-on-a-chip and the kidney', *Kidney Research and Clinical Practice*, 34(3), pp. 165–169. Available at: https://doi.org/10.1016/j.krcp.2015.08.001.

Lelièvre, S.A., Kwok, T. and Chittiboyina, S. (2017) 'Architecture in 3D cell culture: An essential feature for in vitro toxicology', *Toxicology in Vitro*, 45, pp. 287–295. Available at: https://doi.org/10.1016/j.tiv.2017.03.012.

Levey, A.S. and Coresh, J. (2012) 'Chronic kidney disease', *The Lancet*, 379(9811), pp. 165–180. Available at: https://doi.org/10.1016/S0140-6736(11)60178-5.

Lidberg, K.A. *et al.* (2022) 'Serum Protein Exposure Activates a Core Regulatory Program Driving Human Proximal Tubule Injury', *Journal of the American Society of Nephrology : JASN*, 33(5), pp. 949–965. Available at: https://doi.org/10.1681/ASN.2021060751.

Liu, B.-C. *et al.* (2018) 'Renal tubule injury: a driving force toward chronic kidney disease', *Kidney International*, 93(3), pp. 568–579. Available at: https://doi.org/10.1016/j.kint.2017.09.033.

Liyanage, T. *et al.* (2015) 'Worldwide access to treatment for end-stage kidney disease: a systematic review', *The Lancet*, 385(9981), pp. 1975–1982. Available at: https://doi.org/10.1016/S0140-6736(14)61601-9.

Morrissey, K.M. *et al.* (2013) 'Renal Transporters in Drug Development', *Annual Review of Pharmacology and Toxicology*, 53(Volume 53, 2013), pp. 503–529. Available at: https://doi.org/10.1146/annurev-pharmtox-011112-140317.

Nieskens, T.T.G. and Wilmer, M.J. (2016) 'Kidney-on-a-chip technology for renal proximal tubule tissue reconstruction', *European Journal of Pharmacology*, 790, pp. 46–56. Available at: https://doi.org/10.1016/j.ejphar.2016.07.018.

R Core Team (2023). R: A language and environment for statistical computing. R Foundation for Statistical Computing, Vienna, Austria. ISBN 3-900051-07-0, Available at: http://www.R-project.org/

Raghavan, V. *et al.* (2014) 'Shear stress-dependent regulation of apical endocytosis in renal proximal tubule cells mediated by primary cilia', *Proceedings of the National Academy of Sciences*, 111(23), pp. 8506–8511. Available at: https://doi.org/10.1073/pnas.1402195111.

Ritchie, M.E. et al. (2015) 'limma powers differential expression analyses for RNA-sequencing and microarray studies', Nucleic Acids Research, 43(7), p. e47. Available at: https://doi.org/10.1093/nar/gkv007.

Sánchez-Romero, N. *et al.* (2016) 'In vitro systems to study nephropharmacology: 2D versus 3D models', *European Journal of Pharmacology*, 790, pp. 36–45. Available at: https://doi.org/10.1016/j.ejphar.2016.07.010.

Soderland, P. *et al.* (2010) 'Chronic Kidney Disease Associated With Environmental Toxins and Exposures', *Advances in Chronic Kidney Disease*, 17(3), pp. 254–264. Available at: https://doi.org/10.1053/j.ackd.2010.03.011.

Su, H., Lei, C.-T. and Zhang, C. (2017) 'Interleukin-6 Signaling Pathway and Its Role in Kidney Disease: An Update', *Frontiers in Immunology*, 8, p. 405. Available at: https://doi.org/10.3389/fimmu.2017.00405.

Tourovskaia, A. *et al.* (2014) 'Tissue-engineered microenvironment systems for modeling human vasculature', *Experimental Biology and Medicine*, 239(9), pp. 1264–1271. Available at: https://doi.org/10.1177/1535370214539228.

Turner, J.M. *et al.* (2012) 'Treatment of chronic kidney disease', *Kidney International*, 81(4), pp. 351–362. Available at: https://doi.org/10.1038/ki.2011.380.

Van Ness, K.P. *et al.* (2017) 'Microphysiological Systems to Assess Nonclinical Toxicity', *Current protocols in toxicology*, 73, p. 14.18.1-14.18.28. Available at: https://doi.org/10.1002/cptx.27.

Vos, T. *et al.* (2020) 'Global burden of 369 diseases and injuries in 204 countries and territories, 1990–2019: a systematic analysis for the Global Burden of Disease Study 2019', *The Lancet*, 396(10258), pp. 1204–1222. Available at: https://doi.org/10.1016/S0140-6736(20)30925-9.

Waikar, S.S. *et al.* (2016) 'Relationship of proximal tubular injury to chronic kidney disease as assessed by urinary kidney injury molecule-1 in five cohort studies', *Nephrology Dialysis Transplantation*, 31(9), pp. 1460–1470. Available at: https://doi.org/10.1093/ndt/gfw203.

Wang, Y.I. *et al.* (2018) 'Multiorgan Microphysiological Systems for Drug Development: Strategies, Advances, and Challenges', *Advanced Healthcare Materials*, 7(2), p. 1701000. Available at: https://doi.org/10.1002/adhm.201701000.

Weber, E.J. *et al.* (2016) 'Development of a microphysiological model of human kidney proximal tubule function', *Kidney international*, 90(3), pp. 627–637. Available at: https://doi.org/10.1016/j.kint.2016.06.011.

Weber, E.J. *et al.* (2018) 'Human kidney on a chip assessment of polymyxin antibiotic nephrotoxicity', *JCI Insight*, 3(24), p. e123673. Available at: https://doi.org/10.1172/jci.insight.123673.

Wilmer, M.J. *et al.* (2016) 'Kidney-on-a-Chip Technology for Drug-Induced Nephrotoxicity Screening', *Trends in Biotechnology*, 34(2), pp. 156–170. Available at: https://doi.org/10.1016/j.tibtech.2015.11.001.